Investigation on Microstructural and Mechanical Behaviour of Atmospheric Plasma Sprayed Stellite 6 Alloy Coatings on AISI 304 Stainless Steel

Sangita Sarangi
Ajit Kumar Mishra
Seshadev Sahoo (seshadevsahoo@soa.ac.in)
Subhra Bajpai

Research Article

Keywords: Stellite 6 alloy, Coating, Microstructure, Microhardness, Plasma spray, XRD

Posted Date: March 14th, 2022

DOI: https://doi.org/10.21203/rs.3.rs-1433594/v1

Abstract

Stellite 6 alloy has been extensively used in industrial applications to prevent wear and corrosion because of its high strength, high hardness, and corrosion resistance. The wear and frictional properties of a material depend largely on the normal load and hardness of the mating surfaces. Wear resistance characteristics of the material can be improved substantially by reorienting the microstructure of the grain size of the metal along with imparting a higher hardness on the mating surfaces. In the present study, an effort is made to deposit Stellite 6 powder having a regular spherical shape with diameters ranging between 15 μm to 45 μm on an AISI 304 stainless steel substrate without any intermittent layer using an atmospheric plasma spray deposition process. The effect of coating thickness (74 μm, 128 μm, and 215 μm) on metallurgical, morphological, and mechanical characteristics was investigated. Optical microscopy, Scanning Electron Microscopy (SEM), and EDS were employed to study the Stellite 6 coating morphology, and the structural analysis was used to identify the phase formation by using XRD. From the experimental analysis it is observed that, the Stellite 6 coating is uniform and homogenous in nature. Sample coated with Stellite 6 powder having 128 μm coating thickness is exhibiting the best microstructure and mechanical properties as compared to the other two coated samples.

1. Introduction

AISI 304 Stainless steel are more frequently used in aerospace, chemical, and power plant industries because of their superior corrosion resistant properties, but its relatively less hardness and the wear resistance property limit its applications in various sectors [1]. Hence, surface coating procedures are adopted on this Stainless-steel material to improve its mechanical properties as well as the working life of these components. Surface coating is one of the best solutions to reduce wear and corrosion, especially products like hydro turbine blades, exhaust valves in engines, cutting tools, molds, dies, etc. which are functioning in the hostile environment [2–4]. Different types of surface coating procedures such as Plasma Transferred Arc deposition process (PTA), Gas Tungsten Arc Welding Process (GTAW), High-Velocity Oxygen Fuel (HVOF) spraying, and Cold gas spraying are available for the reduction of wear and corrosion, resulting in an improvement in the reliability of such components. Atmospheric plasma spray is also a type of surface coating technique that uses different types of coating powders like ceramic, metallic, polymeric, composite, etc. for coating on any kind of substrate materials [5]. The coating produced by the plasma spray technique has resulted in better corrosion resistance with improving the service life of the substrate materials. In this process, the coating powder is initiated into the thermal plasma jet which gets melted and moved towards the substrate at a very faster rate. These molten droplets are quenched after impact with the substrate forming layered microstructure and may also contain very few defects like pores, splats, and micro cracks. Also, coatings of good quality, adherence with higher deposition efficiency are provided by the plasma spraying technique [6, 7].

Stellite 6 is a Co-based super-alloy broadly used for coating purposes and provides efficient erosion and corrosion-resistant properties at the working temperature above 1095^{o}C [8–10]. The wear and corrosion resistance property of the Stellite 6 coated steel components are increased due to the formation of

carbide. Chromium is the prime element that forms carbides in Stellite 6 alloys and enhances the wear-resistant property of the Stellite 6 coated steel. It also forms chromium oxide as a protective layer to safeguard the Stellite 6 coated steel from oxidation. Wang et al. [11] found that the addition of yttrium in Stellite alloys improved the wear performance at 650^{o}C. The carbides of type $Cr_7C_3$was the main carbide found in high carbon Stellite and carbides like Cr_6C and $Cr_{23}C_6$ were identified in low carbon Stellite. Due to the presence of these carbides in the matrix, hardness gets imparted on the coated surfaces resulting in an improvement in wear resistance properties [12]. The wear performance of Stellite coated steel substrate gets influenced by the mechanical and metallurgical properties of the carbides [13]. The wear performance of Stellite coated AISI 1045 carbon steel by plasma transferred arc deposition method was increased due to the formation of M_6Ctype carbides [14]. Budzynski et al. [15] investigate the tribological behavior of Stellite 6 alloy with ion implantation. Their study mostly focused on the effect of nitrogen ion implantation to change the properties of the Stellite 6 alloy, but there is lacking the systemic study on Stellite 6 alloy. Thawari et al. [16] produced a wear-resistant Stellite 6 coating with the crack-free layer in the laser cladding method and investigated the mechanical and microstructural properties by adding a buffer layer. The authors found that Stellite coating with buffer layer has shown promising results as compared to without buffer layer. The mechanical, microstructural, and tribological properties of Stellite coated Stainless steel was investigated by Jeyaprakash et al. [17]. From this investigation, the authors observed that Stellite 6 coating has shown a dendritic structure due to rapid cooling which increases the hardness of the coatings. The effects of process parameters on mechanical and tribological properties of Stellite-6coatings obtained by Cold Gas Dynamic Spray and High-Velocity Oxy-Fuel Spray were investigated by Magaro et al. [18] and Sassatelli et al. [19] respectively. The authors tried to address some of the technical issues with the process and studied the microstructural and mechanical properties. Based on their study the processing conditions were optimized. Lima et al. [20] investigated different coating technology on the properties like microstructure, mechanical, wear, and corrosion properties of the Stellite 6 coatings and found that High-Velocity Oxy-Fuel coating shown better properties than Gas Tungsten Arc Welding hot-wire cladding.

Previous studies indicate that a large number of physical and chemical processes were available to increase the hardness of the surfaces increasing wear-resistant properties. However, there was a lacking of a systematic approach to investigate the behavior of Stellite 6 coating on AISI 304 Stainless Steel by the atmospheric plasma spray process. Also, the combination of coating thickness coupled with hardness and microstructure of the material was less investigated. In the present study, efforts have been made to coat the AISI 304 Stainless Steel substrate with Stellite 6 powder using the atmospheric plasma spray technique by varying the coating thickness and investigating the structural and mechanical properties. The effect of various coating thicknesses on their mechanical behavior along with morphological characteristics is investigated for optimizing the coated product.

2. Materials And Experimental Details

2.1 Materials

Austenitic grade AISI 304 Stainless Steel is widely used in industry as structural steel. Three samples having dimensions of 100mm x 60mm x3mm were selected as the substrate material for coating and conducting subsequent experiments. The chemical composition of the substrate material in wt% is shown in Table 1. The commercially available AISI 304 Stainless Steel plate has a surface finish of 1 µm and 3 µm. Before undertaking the coating process, surface preparation of the substrate material was done by cleaning the surfaces of the plates with acetone. Alumina grit blasting was done with a grit size of 400 µm on AISI 304 Stainless Steel substrate to enhance the surface roughness of 5µm that ameliorates mechanical interlocking between the substrate and coating.

Cobalt-based Stellite 6 powder was taken as a coating material on AISI 304 Stainless Steel substrate as it exhibits excellent corrosion and wears resistant properties. The particle size distribution of the powder was measured using the laser diffraction technique and it is found that the nominal particle size distribution of the powder was between 15 µm to 45µm. The chemical composition of the Stellite 6 powder as supplied was determined using an Optical Emission Spectrometer (OES) and the findings are shown in Table 1. The Stellite 6 powder is used as the feedstock powder for coating the steel substrate through the atmospheric plasma spraying process.

Table 1
Chemical composition of AISI 304 stainless steel and Stellite 6 powder

AISI 304		**Stellite 6**	
Element	**Wt.%**	**Element**	**Wt.%**
Cr	18.736	Co	57.822
Ni	8.288	Cr	32.273
Si	0.366	W	4.7909
Mn	1.440	Ni	2.4611
C	0.023	Fe	1.1275
S	0.006	Mo	0.2956
P	0.029	C	0.98
Fe	Balance	Si	0.95
		Mn	0.2281
		Nb	0.005

2.2. Sample preparation and characterization

A MEC MPS-50M type plasma gun with PS-50 plasma power source was employed in plasma spraying of Stellite 6 for coating. The Stellite 6 powder as feedstock material was injected into the plasma jet produced using argon and hydrogen gases. The carrier gas (Ar) transports the powder from the powder

feeder unit to the plasma plume which also inhibits oxidation. The process parameters for the plasma spraying process are listed in Table 2. The parameters used in the spraying process are kept constant throughout the experiment. The coating on the substrate is done using a robot with application software. The coating is accomplished by depositing the powder layer by layer on the steel substrate by longitudinal and transverse deposition weaving technique alternately.

Table 2
Plasma spray process parameter for spraying Stellite 6 powder

Parameters	Value
Current(A)	500
Voltage (V)	43.1
Power (Kw)	21.4
Primary gas (Ar) flow rate(l/min)	40
Secondary gas (H_2) flow rate(l/min)	0.2
Carrier gas (Ar) flow rate(l/min)	5
Primary feeder plate (RPM)	4
Nozzle to substrate distance (mm)	110

The coating density was calculated by peeling a small portion from the surface of the substrate by mechanical means. Archimedes principle is used for the determination of density. Surface roughness and adhesion test were performed to know the roughness of the coating surface and bonding strength of the coating with substrate respectively. The Stellite 6 coated stainless-steel samples were bisected and cold mounted for microscopy analysis. The mounted samples were polished with different emery paper with required chemicals, then cleaned and dried properly to reveal the microstructure using optical microscopy and SEM. Various phases present in the powder and the coatings were investigated using an X-ray Diffractometer with CuKα (λ = 1.5406 Å) 40 mA. The scanning angle range was varied from 10° to 80°, by a step width of 0.02 and 5 s time per step. The surface morphology of powder and coating were analyzed using the scanning electron microscope, equipped with Energy Dispersive X-ray Spectroscopy (EDS) for elemental analysis at different phases. The microhardness of the coating measurement was made using a Vickers microhardness tester. A load of 300 g was maintained throughout the experiments for a time duration of 10 s.

3. Results And Discussions

3.1. Characterization of Stellite 6 powder

The commercially procured Stellite 6 powder is characterized by Scanning electron microscopy (SEM) and the morphology of the powder is shown in Fig. 1(a). The micrograph shows that most of the particles are spherical with regular shapes with little agglomeration seen for smaller size particles. Agglomeration of particles sometimes takes place leading to a variation in shape. More ever, very few fragmented particles are also existing. Therefore, with the presence of regular shape particles, the coating produced by Stellite 6 powder is generally smooth and homogenous. Figure 1(b) shows the particles size distribution and the size concentration. It is found that the size range of particles lies between 18 μm to 34 μm. It has a peak value of 25 μm with a Gaussian distribution of 8.18. This value indicates around 25μm is the film thickness that will be obtained in a single pass at the time of coating. X-Ray Diffraction pattern of Stellite 6 powder is shown in Fig. 1(c). It is evident from the diffraction pattern that the powder consists of a Co-based solid solution with prominent peaks. It has very low peaks with uniform distributions of prominently Cr_7C_3 carbide phase. Cobalt possesses a hexagonal closed pack structure at room temperature [21]. The Stellite 6 powder is normally produced by spray drying and the atomization process. During the atomization process, a high cooling rate is experienced, due to which a low amount of Cr_7C_3 carbide is observed. This finding is also corroborated [22].

3.2. Calculation of Coating thickness and Adhesion Strength

Coating of Stellite 6 powder on the vertically held steel substrate is carried out in a layered approach through passes with longitudinal and transverse direction and a 25 μm thickness of the coating is obtained in every pass. An optical micrograph image of the plasma-spray coated Stellite 6 on AISI 304 Stainless steel substrate is shown in Fig. 2. From the micrograph three distinct layers are observed i.e., the first layer (marked 1) is the bottom layer depicts SS 304 steel substrate, intermittent layer (marked 2) represents the coated surface, and the top layer (marked 3) is the resin. The Stellite 6 powder coating was deposited in a lamellar texture. It is found that sample 3 depicts the most uniform coating thickness whereas sample 1 has an irregular coating thickness as compared with all three micrographs. Average coating thickness as measured from the micrographs is 74 μm, 128 μm, and 215 μm for 1st, 2nd, and 3rd samples and the variation in coating thickness ranges between 38.43%, 20.23%, and 7.69% respectively. It can be inferred that without changing the process parameters for atmospheric plasma spray deposition technology larger coated products exhibit a sound and smooth coating. Large particles associated with the powders are melted instantly, incur rapid solidification, and get deposited uniformly in the wall of the substrate. This phenomenon could not be witnessed while depositing the coating material on the lower coating thickness products.

The adhesion tests were performed on the 100 mm x 60 mm sample size with an automatic adhesion tester. The Adhesion dolly with a circular contact surface of 10 mm diameter has adhered with sample with adhesive HTK ultra-bond 100 after proper surface cleaning with emery and acetone. Assembled system is then put into an oven at 150˚C for 80 minutes for the curing of the adhesive and to strengthen the bond of the dolly with the coated surface. The parting of the coating has taken place at the interface (coalition) of the coating and substrate which is shown in Fig. 3. In all three samples, adhesion pull-up

strength has a magnitude varying between 26.5 ± 2MPa corresponding to strong intra-bonding in Stellite particles. Also evident from the fractured surface, a negligible amount of coating has been pulled out from the coating. In the case of sample 3 having 215μmcoatings thickness, the adhesion strength value is beyond 28 MPa, showing an appreciable amount of visible coating pull-out. The strength obtained in adhesion testing is considered good because of more no of touchpoints between the well-flattened splats.

3.3. Density, Porosity, and Surface Roughness of Stellite 6 coating

The coating density is calculated by peeling a small portion from the surface of the substrate by mechanical means. Archimedes principle [23] as shown in Eq. (1) is used for the determination of density.

$$Densityofthecoating = d_w \times \frac{M_a}{\left(M_a - M_w\right)} \quad (1)$$

where d_w is the density of water, M_a is the weight of the coated sample in the air (gm), M_w is the weight of the coated sample in water (gm). Material with higher coating density indicates a superior and homogeneous coating justifying a superior load requirement for its delamination and removal leading to failure.

Physical parameters such as density, porosity, and surface roughness are depicted in Table3. The density of Stellite 6 is reported as 8.69 g/cm^3. The calculated value of the density of the coating was 8.44 g/cm^3. Optical microscopic image analysis (OMIA) techniques were used for the determination of the homogeneity of the coating. The porosity of coated samples was calculated by Image J processing and analysis software. Ten different observations are taken at different locations and the porosity of the coated surface is calculated using the statistical average method. The porosity value for the plasma sprayed coating is found to be in the range of 2.9 ± 0.05%. Sidhu et al. [24] observed the porosity of plasma-sprayed Stellite 6 coating lies between 2-3.5%. From the table, it is observed that sample 2 has the lowest porosity value.

The surface roughness of the coated product was measured using a surface roughness instrument. Five roughness readings are taken on each sample and their average value is taken as the surface roughness. The coated product surface roughness value for all the samples is measured using a surface roughness meter and its roughness values vary between 4.8 ± 0.02 μm. The average value of surface roughness for HVOF sprayed Stellite 6 coating on various grades of steel substrates lies in the range of 4.892 ± 0.38 μm [25]. The atmospheric plasma spray technique has resulted in a better surface finish as compared to the HVOF process in depositing Stellite 6 powder on stainless steel substrates.

Table 3
Density, porosity, and surface roughness of the Stellite 6 coated samples

Samples	Coating thickness	Density	Porosity	Surface roughness
Sample-1	74 μm	8.44gm/cm^3	2.95%	4.78 μm
Sample-2	128 μm	8.44gm/cm^3	2.85%	4.8 μm
Sample-3	215 μm	8.44gm/cm^3	2.90%	4.82 μm

3.4. Phase analysis of Stellite 6 coating

Figure 4 shows the XRD pattern of the Stellite 6 coating. From the XRD plot, it is observed that the structure of the coating consists of cobalt solid solution along with $Cr_{23}C_6$, Cr_7C_3andCrO. At the highest peak intensity, the carbides of Chromium ($Cr_{23}C_6$ and Cr_7C_3), coincides with the Co-based matrix. Due to instant cooling after deposition of the powder on SS 304 steel plate during atmospheric plasma spray process, cobalt fails to undergo the alteration of equilibrium phase, thus permitting to remain in FCC structure consistent with the temperature exceeding417^{0}C [26]. There is also a small peak of CrO from the XRD pattern. The presence of CrO indicates that some oxidation of chromium might have taken place during the plasma spraying process.

3.5. Analysis of coating microstructure

Figure 5 shows the SEM image of the plasma sprayed Stellite 6 coating on the AISI304 substrate. It is observed that two different phases are visible from the micrograph. The dark grey phase corresponds to structure 1 enriched with Chromium which is also called as inter-dendritic eutectic phase and the light grey region corresponds to structure 2 enriched with Cobalt called a dendritic phase. This interdendritic eutectic phase consists of Cobalt with Chromium carbide [27, 28] and the dendritic phase consists of Cobalt solid solution (FCC structure). Solid solution hardening and precipitates of carbides play a great role to provide strength to the cobalt-based superalloy. It is also observed from XRD that Chromium is the main element forming carbide during the coating process. It also improves the solid solution hardening along with resistance to corrosion and oxidation. The carbides like$Cr_{23}C_6$ and $Cr_7C_3$are formed by Cr. But due to the metastable nature of Cr_7C_3 sometimes it converts into $Cr_{23}C_6$during a higher temperature working environment [29].

The corresponding EDS analysis of different structures (marked as 1 and 2 in micrograph) in all the samples is presented in Fig. 7 and Table 4. From this table, it is found that Co, Cr, and W are the dominant element in the dendritic as well as the interdendritic region. Oxygen is present in the interdendritic region in an abundant manner mostly due to SiO_2. Also, it is observed that there is the presence of splats, partially melted and un-melted particles in the form of voids, pores, or globules in the coatings which are the characteristic feature of plasma spray coatings. These pores or voids which are marked from SEM and optical micrographs are black. Some oxides of Cr appear as thin dark (black) phases and are located

as a marginal line between the laminas. These are formed instantly after the deposition process due to the reaction of lamellae with the adjacent air [30, 31]. When W and Mo are present in the microstructure of Stellite 6 they provide strength by forming carbides or intermetallic compounds [27, 29]. But the presence of W from EDS elemental mapping analysis is very less as compared with Co and Cr. So, there is no presence of white phase which is enriched with tungsten as seen from PTA coated surfaces [32, 33]. Hence it is assumed that tungsten is embedded in the cobalt matrix within the interdendritic phase and provides additional strength employing solid solution hardening.

Table 4
EDS analysis of Stellite 6 coatings

Samples	Marked region in the micrograph	Co	Cr	W	Fe	C	O	Si
Sample 1	1	56.71	29.64	6.58	2.32	4.75	—	—
	2	21.02	57.02	2.16	—	—	18.53	1.27
Sample 2	1	62.74	23.07	5.48	1.91	6.18	0.61	—
	2	16.26	51.54	2.21	—	6.09	22.45	1.45
Sample 3	1	57.29	30.82	3.89	1.35	4.94	0.3	1.4
	2	16.45	57.11	3.36	—		23.08	—

3.6. Analysis of microhardness

Figure 7 shows the microhardness values of the coated materials undertaken on SS 304 substrate. The substrate material has an average microhardness value of 163 $HV_{0.3}$. Sample1 exhibits the lowest hardness of 315 $HV_{0.3}$ as compared to the other samples. The Microhardness of sample 2, sample 3 is nearly identical. As the coating thickness of sample 1 is very small so it gets punctured thus reflecting the hardness of the substrate. Yu et al., [34], reported that the hardness value of (402.6 ± 20.9 $HV_{(2.94\ N)}$ was obtained for the Stellite6 materials produced through sand casting.

4. Conclusion

Stellite 6 powder was successfully deposited on AISI 304 stainless steel substrate by atmospheric plasma spray process without any intermittent bond coat. 25 microns of coating thickness was obtained in a single pass adopting longitudinal and transverse (weaving) deposition process. Three stainless steel plate samples were coated on a single flat surface, having 74 µm, 128 µm, and 215 µm coating thickness. Coated surface was smooth and homogeneous for higher coating thickness. The adhesion strength between the substrate and coating was obtained between 26.5 ± 2 MPa indicating a uniform strength for coated products. Sample coated with Stellite 6 powder having 128 µm coating thickness is exhibiting the best microstructure and mechanical properties as compared to the other two coated samples.

Declarations

Acknowledgments

The authors are grateful to the Director, CSIR-Institute of Minerals and Materials Technology (CSIR-IMMT), Bhubaneswar for providing necessary support for conducting this research work.

Funding: *The authors declare that no funds, grants, or other support were received during the preparation of this manuscript.*

Competing Interests: *The authors have no relevant financial or non-financial interests to disclose*

Author Contributions: *All authors contributed to the study conception and design. Material preparation, data collection and analysis were performed by Sangita Sarangi. The first draft of the manuscript was written by Sangita Sarangi, and Ajit Kumar Mishra and all authors commented on previous versions of the manuscript. All authors read and approved the final manuscript.*

Data Availability: *The datasets generated during and/or analysed during the current study are available from the corresponding author on reasonable request.*

References

1. V.H. Hidalgo, J.B. Varela, A.C. Menendez, S.P. Martinez, High temperature erosion wear of flame and plasma-sprayed nickel–chromium coatings under simulated coal-fired boiler atmospheres. Wear **247**, 214–222 (2001)
2. R. Ahmed, A. Ashraf, M. Elameen, N.H. Faisal, A.M. El-Sherik, Y.O. Elakwah, M.F.A. Goosen, Single asperity nano scratch behavior of HIPed and cast Stellite 6 alloys. Wear **312**(1–2), 70–82 (2014)
3. S. Apay, B. Gulenc, Wear properties of AISI 1015 steel coated with Stellite 6 by microlaser welding. Mater. Design **55**, 1–8 (2014)
4. J.V. Giacchi, C.N. Morando, O. Fornaro, H.A. Palacio, Microstructural characterization of as-cast biocompatible Co–Cr–Mo alloys. Mater. Charact. **62**(1), 53–61 (2011)
5. L. Pawlowski, *The science and engineering of thermal spray coatings* (John Wiley & Sons, 2008)
6. G. Di Girolamo, A. Brentari, C. Blasi, E. Serra, Microstructure and mechanical properties of plasma sprayed alumina-based coatings. Ceram. Int. **40**(8), 12861–12867 (2014)
7. M.A. Zavareh, A.A.D.M. Sarhan, B.B. Abd Razak, W.J. Basirun, Plasma thermal spray of ceramic oxide coating on carbon steel with enhanced wear and corrosion resistance for oil and gas applications. Ceram. Int. **40**(9), 14267–14277 (2014)
8. S.S. Chang, H.C. Wu, C. Chen, Impact wear resistance of stellite 6 hardfaced valve seats with laser cladding. Mater. Manuf. Processes **23**(7), 708–713 (2008)
9. F. Luo, A. Cockburn, R. Lupoi, M. Sparkes, W. O'Neill, Performance comparison of Stellite 6® deposited on steel using supersonic laser deposition and laser cladding. Surf. Coat. Technol. **212**,

119–127 (2012)

10. W.C. Lin, C. Chen, Characteristics of thin surface layers of cobalt-based alloys deposited by laser cladding. Surf. Coat. Technol. **200**(14–15), 4557–4563 (2006)
11. L. Wang, D.Y. Li, Effects of yttrium on microstructure, mechanical properties and high-temperature wear behavior of cast Stellite 6 alloy. Wear **255**(1–6), 535–544 (2003)
12. M. Sebastiani, V. Mangione, D. De Felicis, E. Bemporad, F. Carassiti, Wear mechanisms and in-service surface modifications of a Stellite 6B Co–Cr alloy. Wear **290**, 10–17 (2012)
13. A. Gholipour, M. Shamanian, F. Ashrafizadeh, Microstructure and wear behavior of stellite 6 cladding on 17 – 4 PH stainless steel. J. Alloys Compd. **509**(14), 4905–4909 (2011)
14. J.C. Shin, J.M. Doh, J.K. Yoon, D.Y. Lee, J.S. Kim, Effect of molybdenum on the microstructure and wear resistance of cobalt basedStellitehardfacing alloys. Surf. Coat. Technol. **166**(2–3), 117–126 (2003)
15. P. Budzynski, M. Kaminski, M. Turek, M. Wiertel, Impact of nitrogen and manganese ion implantation on the tribological properties of Stellite 6 alloy, Wear 456–457 (2020) 203360
16. C. Nikhil Thawari, J.K. Gullipalli, T.V.K. Katiyar, Gupta, Influence of buffer layer on surface and tribomechanical properties of laser cladded Stellite 6. Mater. Sci. Eng., B **263**, 114799 (2021)
17. N. Jeyaprakash, Che–Hua Yang, Sheng–Po Tseng, Wear Tribo–Performances of Laser Cladding Colmonoy–6 and Stellite–6 Micron Layers on Stainless Steel 304 Using Yb:YAG Disk Laser. Met. Mater. Int. **27**, 1540–1553 (2021)
18. P. Magaro, A.L. Marino, A. Di Schino, F. Furgiuele, C. Maletta, R. Pileggi, E. Sgambitterra, C. Testani, M. Tului, Effect of process parameters on the properties of Stellite-6 coatings deposited by Cold Gas Dynamic Spray. Surf. Coat. Technol. **377**, 124934 (2019)
19. G. Paolo Sassatelli, M.L. Bolelli, Gualtieri, EsaHeinonen,Mari Honkanen, L., Lusvarghi, TizianoManfredini, Rinaldo Rigon, MinnamariVippola, Wear and corrosion performance of Stellite 6® coatings applied by HVOF spraying and GTAW hotwire cladding, Journal of Materials Processing Tech. 284 (2020) 116734
20. C.R.C. Lima, M.J.X. Belém, H.D.C. Fals, C.A. Della Rovere, Wear and corrosion performance of Stellite 6® coatings applied by HVOF spraying and GTAW hotwire cladding. J. Mater. Process. Tech **284**, 116734 (2020)
21. D.P. Dinega, M.G. &Bawendi, A solution-phase chemical approach to a new crystal structure of cobalt. AngewandteChemie Int. Ed. **38**(12), 1788–1791 (1999)
22. F. Duflos, J.F. Stohr, Comparison of the quench rates attained in gas-atomized powders and melt-spun ribbons of Co- and Ni-base superalloys: influence on resulting microstructures. J. Mater. Sci. **17**, 3641–3652 (1982)
23. Sweta Rani Biswal, & Seshadev Sahoo, Fabrication of WS2 Dispersed Al-BasedHybrid Composites Processed by PowderMetallurgy: Effect of Compaction Pressure and Sintering Temperature. J. InorgOrganometPolym **30**, 2971–2978 (2020)

24. B.S. Sidhu, S. Prakash, Studies on the behavior of stellite-6 as plasma sprayed and laser remelted coatings in molten salt environment at 900 C under cyclic conditions. J. Mater. Process. Technol. **172**(1), 52–63 (2006)
25. H.S. Sidhu, B.S. Sidhu, S. Prakash, Solid particle erosion of HVOF sprayed NiCr and Stellite-6 coatings. Surf. Coat. Technol. **202**(2), 232–238 (2007)
26. X. Men, F. Tao, L. Gan, F. Zhao, Z. Xu, Erosion behavior and surface cracking mechanism of Co-based coating deposited via PTA under high-speed propellant airflow. Surf. Coat. Technol. **372**, 369–375 (2019)
27. T. Lolla, J. Siefert, S.S. Babu, D. Gandy, Delamination failures of Stellitehardfacing in power plants: a microstructural characterization study. Sci. Technol. Weld. Join. **19**, 476–486 (2014)
28. R. Singh, D. Kumar, S.K. Mishra, S.K. Tiwari, Laser cladding of Stellite 6 on stainless steel to enhance solid particle erosion and cavitation resistance. Surf. Coat. Technol. **251**, 87–97 (2014)
29. D. Klarstrom, J. Wu (2004). Metallography and microstructures of cobalt and cobalt alloys. *Materials Park, OH: ASM International, 2004.*, 762–774
30. S. Deshpande, S. Sampath, H. Zhang, Mechanisms of oxidation and its role in microstructural evolution of metallic thermal spray coatings - case study for Ni-Al. Surf. Coat. Technol. **200**, 5395–5406 (2006)
31. A.H. Dent, A.J. Horlock, D.G. McCartney, S.J. Harris, Microstructural characterization of a Ni-Cr-BC based alloy coating produced by high velocity oxy-fuel thermal spraying. Surf. Coat. Technol. **139**(2–3), 244–250 (2001)
32. M.S. Sawant, N.K. Jain, Investigations on wear characteristics of Stellite coating by micro-plasma transferred arc powder deposition process. Wear **378**, 155–164 (2017)
33. X. Men, F. Tao, L. Gan, F. Zhao, Z. Xu, Erosion behavior and surface cracking mechanism of Co-based coating deposited via PTA under high-speed propellant airflow. Surf. Coat. Technol. **372**, 369–375 (2019)
34. H. Yu, R. Ahmed, H.D.V. Lovelock, S. Davies, Influence of manufacturing process and alloying element content on the tribomechanical properties of cobalt-based alloys. J. Tribol. **131**(1), 011601 (2009)

Figures

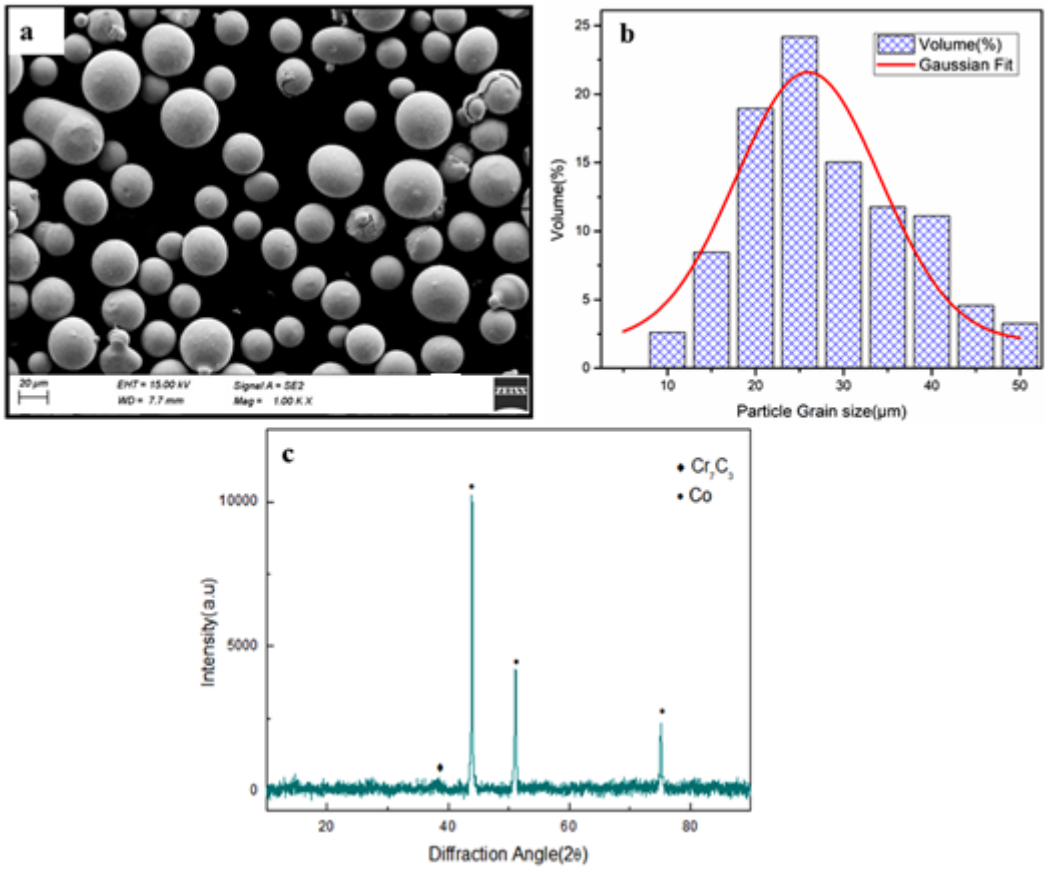

Figure 1

(a) SEM micrograph of Stellite 6 powder, (b) Particle size distribution, and (c) XRD plot of Stellite 6 powder

Figure 2

Optical Micrograph of the as-coated Stellite 6 on Stainless Steel substrate (a) for sample 1, (b) for sample 2, (c) for sample 3 (1= substrate, 2= Stellite 6 coating, 3=resin)

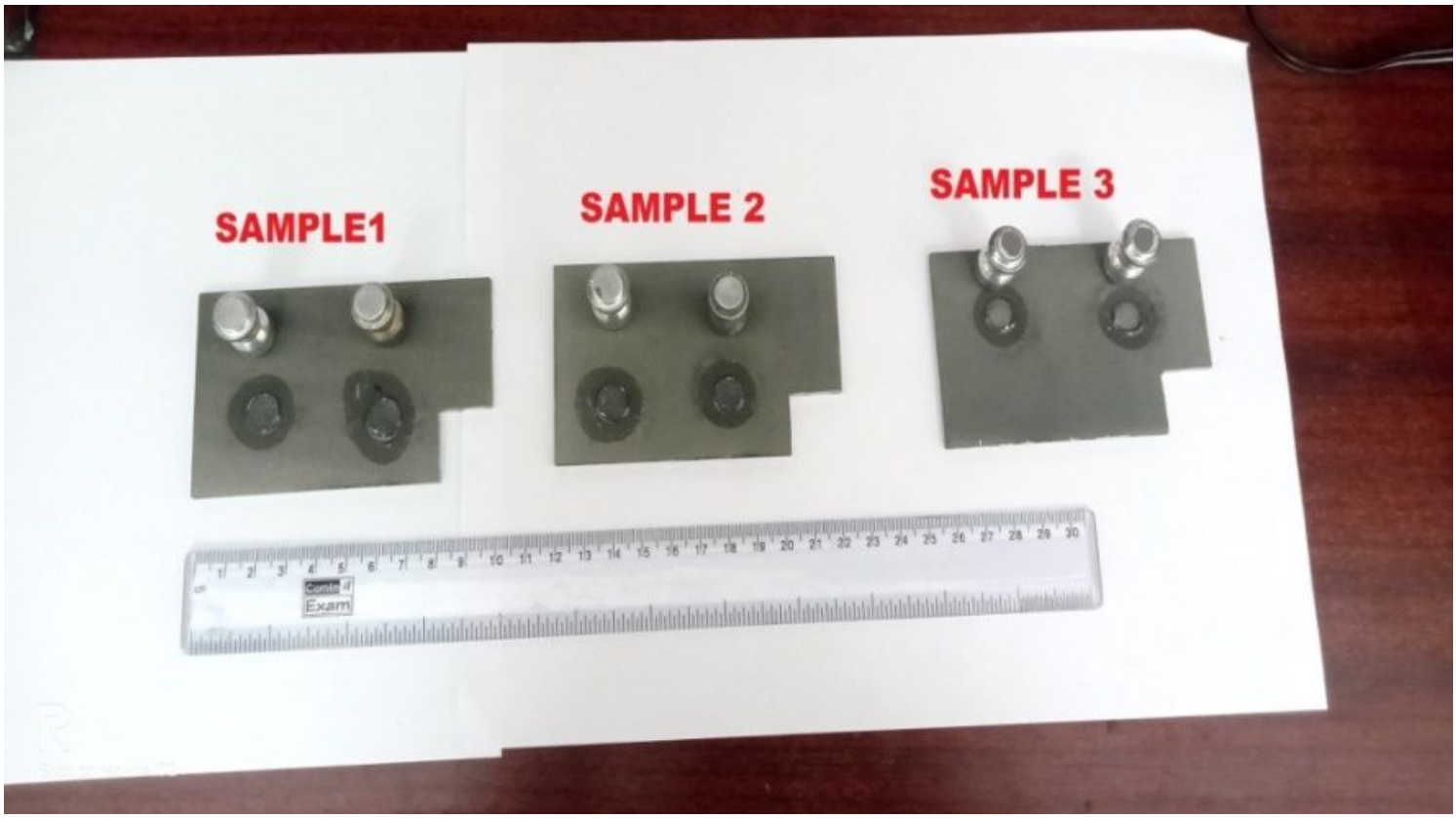

Figure 3

Adhesion tested Samples

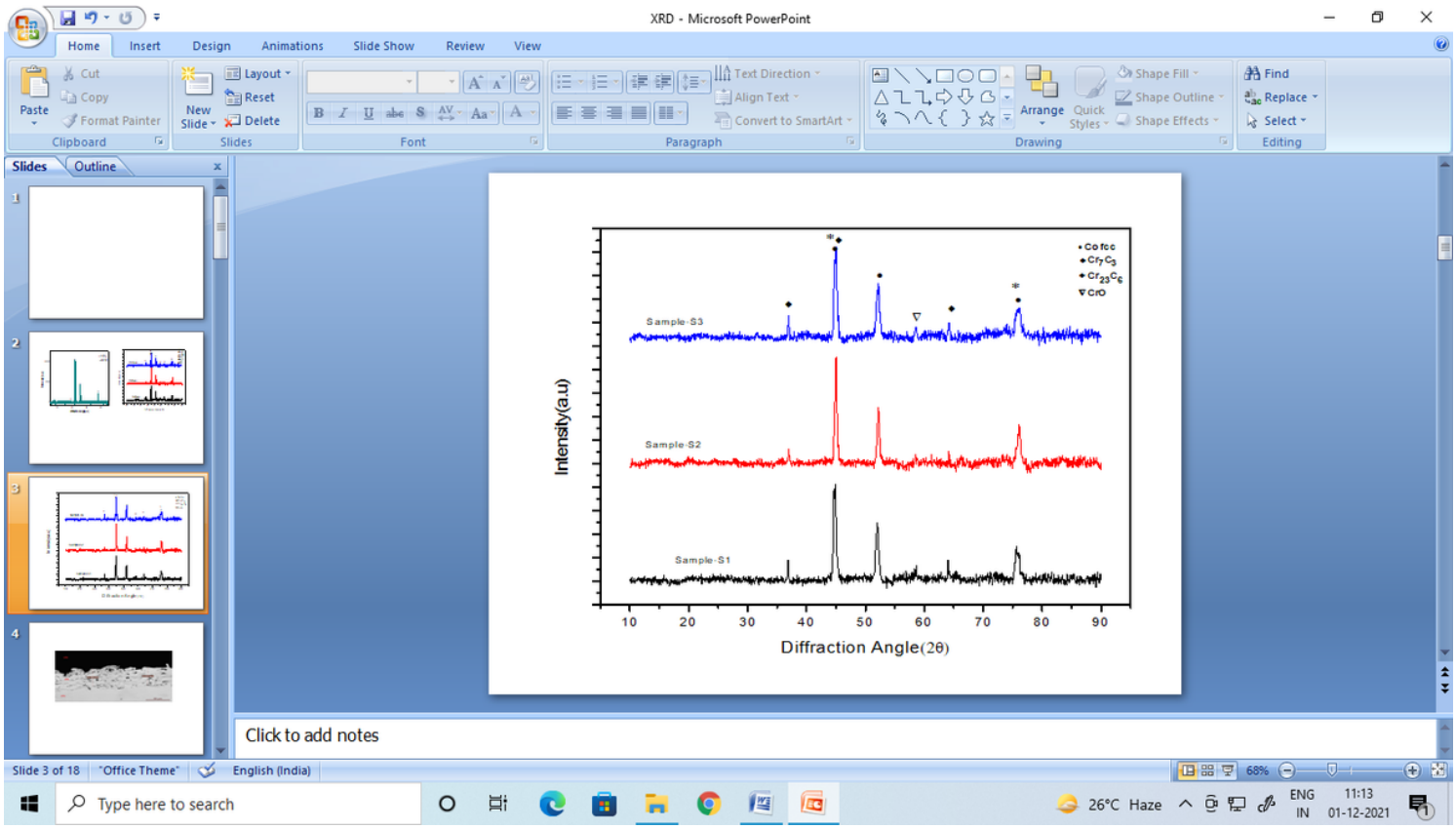

Figure 4

XRD pattern of Stellite 6 coating

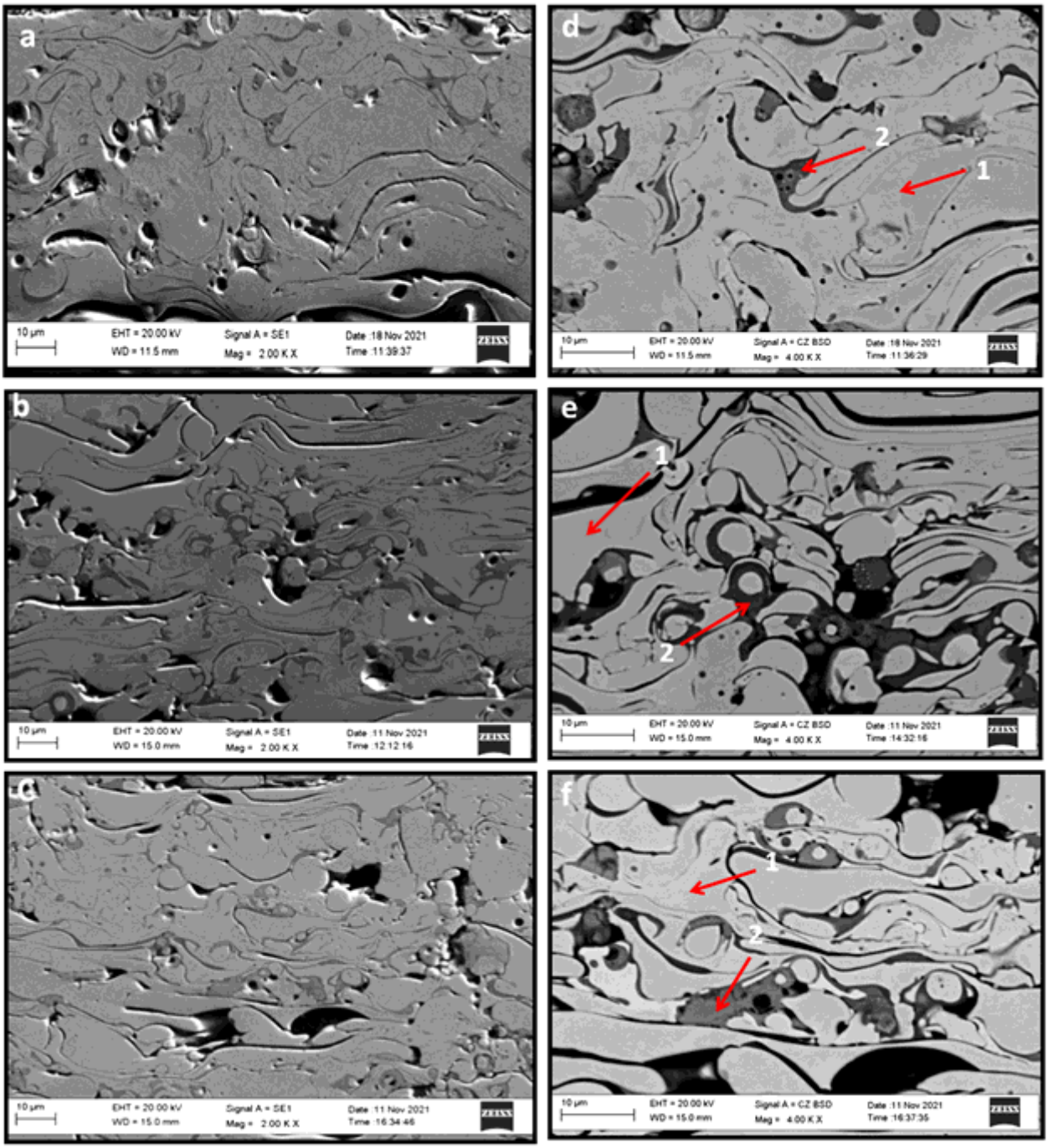

Figure 5

SEM micrograph of Stellite 6 coatings at different magnification (a), (d) sample1, (b), (e) sample 2 and (c), (f) sample 3

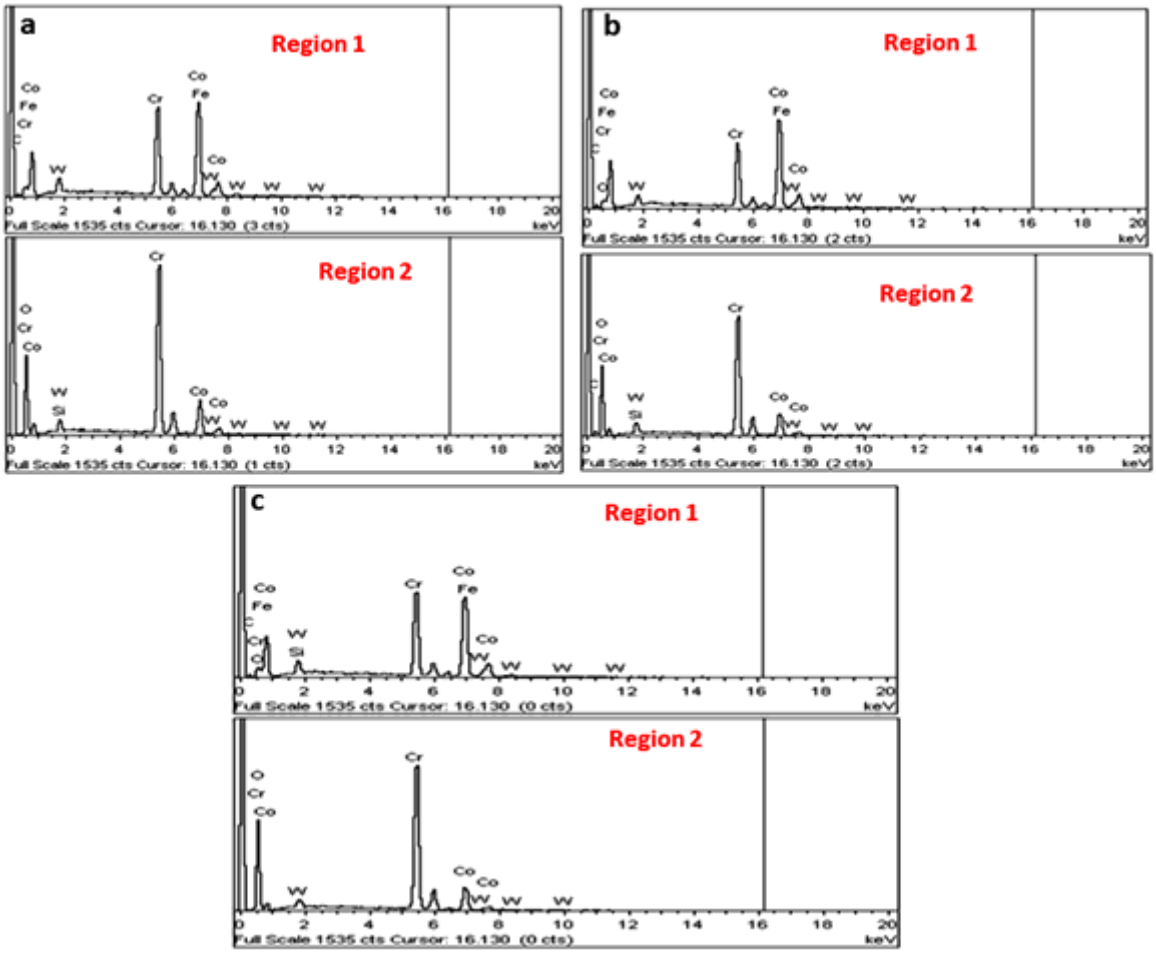

Figure 6

EDS analysis of different structures in (a) Sample1 (b) Sample 2 (c) Sample 3

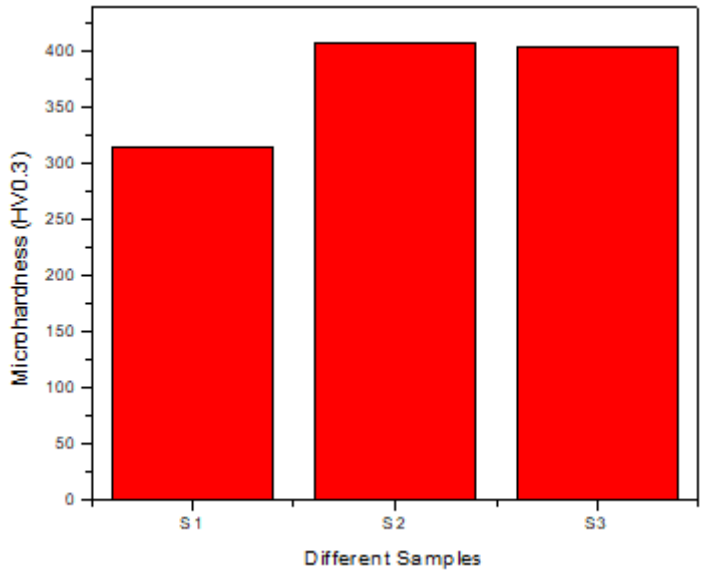

Figure 7

Microhardness of different coated samples